



## City Research Online

### City, University of London Institutional Repository

---

**Citation:** Zhang, Z., Wu, Y., Jia, M., Song, H., Sun, Z., Zong, H. & Li, Y. (2017). The multichannel discharge plasma synthetic jet actuator. *Sensors and Actuators A: Physical*, 253, pp. 112-117. doi: 10.1016/j.sna.2016.11.011

This is the accepted version of the paper.

This version of the publication may differ from the final published version.

---

**Permanent repository link:** <https://openaccess.city.ac.uk/id/eprint/16926/>

**Link to published version:** <https://doi.org/10.1016/j.sna.2016.11.011>

**Copyright:** City Research Online aims to make research outputs of City, University of London available to a wider audience. Copyright and Moral Rights remain with the author(s) and/or copyright holders. URLs from City Research Online may be freely distributed and linked to.

**Reuse:** Copies of full items can be used for personal research or study, educational, or not-for-profit purposes without prior permission or charge. Provided that the authors, title and full bibliographic details are credited, a hyperlink and/or URL is given for the original metadata page and the content is not changed in any way.

---

---

---

City Research Online:

<http://openaccess.city.ac.uk/>

[publications@city.ac.uk](mailto:publications@city.ac.uk)

---

# The multichannel discharge plasma synthetic jet actuator

Zhibo ZHANG<sup>1</sup>, Yun WU<sup>1,2\*</sup>, Min JIA<sup>1</sup>, Huimin SONG<sup>1</sup>,  
Zhengzhong SUN<sup>3</sup>, Haohua ZONG<sup>2</sup>, Yinghong LI<sup>1</sup>

1 Science and Technology on Plasma Dynamics Laboratory, Air Force Engineering University, Xi'an, 710038, People's Republic of China

2 Science and Technology on Plasma Dynamics Laboratory, Xi'an Jiaotong University, Xi'an, 710049, People's Republic of China

3 Department of Mechanical Engineering and Aeronautics, City University London, London, United Kingdom

Corresponding author: Yun WU, wuyun1223@126.com

**Abstract:** The plasma synthetic jet actuator (PSJA) is a flow control device capable of generating high speed pulsed jet. However, the performance of conventional PSJA is restricted by low discharge efficiency and small control area, because one power supply only drives one electrode couple. The present work is to propose a new concept of multichannel discharge plasma synthetic jet actuator (MD-PSJA), which is driven by single power supply. The new MD-PSJA has two types, namely the multi-electrode PSJA and the multi-PSJA array. These two types of MD-PSJA are examined experimentally. The multi-electrode PSJA containing 11-electrode PSJA is first studied. Comparison with standard 2-electrode PSJA reveals that the discharge efficiency and jet velocity increase 200% and 47% respectively under the same input energy and discharge voltage. The multi-PSJA array is later evaluated. One power supply is found to be able to drive an array of 12 PSJAs, resulting in 6 times affected area and 64% jet velocity of a conventional PSJA. The proposed MD-PSJA is finally concluded an improved active flow control actuator in high speed applications.

**Keywords:** multichannel discharge; spark jet actuator; plasma synthetic jet actuator; PSJA array; plasma flow control

## 1. Introduction

Plasma actuator is an attractive type of active flow control technique due to the absence of moving components, fast response and wide bandwidth <sup>[1,2]</sup>. The dielectric barrier discharge (DBD) plasma actuator and arc discharge actuator are two typical plasma actuators.

The DBD plasma actuator is usually comprised of two flat electrodes flush mounted on either side of a dielectric <sup>[3,4]</sup>. Recent research found that the thin exposed electrode of DBD actuator has the benefit of higher moment transfer to air <sup>[5,6]</sup>. Substantial efforts have been made to improve the performance of the DBD type actuator. Several configurations were proposed to increase the induced velocity. One actuator features multi-electrodes in serial arrangement <sup>[7]</sup>, while there is also DBD actuator with three-electrode <sup>[8]</sup>. Three-dimensional vortical structure can also be produced through DBD actuators through realignment of the electrodes in to shapes of triangle, serpentine and square <sup>[9]</sup>. In some applications, the electrodes are arranged into annular configuration to generate a vertical jet. This DBD actuator is also named plasma synthetic jet actuator (PSJA) <sup>[10,11]</sup>. Despite the great performance improvement of DBD actuator, its induced flow velocity is still low at present, usually less than 10m/s <sup>[12,13]</sup>. This deficit restricts its application in supersonic flow control.

The arc discharge (AD) actuator is different from the DBD actuator. The anode and cathode of the AD actuator are installed on the same surface. For the AD actuator, the joule heating by arc discharge is nontrivial and is considered as an important actuation mechanism, which results in strong shock wave [14]. To take advantage of the fast joule heating, Cybyk et al. put forward a new type of arc discharge actuator with name of plasma synthetic jet actuator (PSJA) (also named spark jet actuator or pulsed plasma jet actuator) [15,16]. In PSJA, the discharge happens in a small cavity instead of an open space. As a result, a high-speed pulsed jet is generated at the outlet orifice. The high speed jet delivered by PSJA makes it suitable for high-speed flow control [17-19].

Limitations of PSJA are gradually identified. It has been found that the overall efficiency of PSJA is low, typically less than 10% [20,21]. The working cycle of PSJA consists of three stages: energy deposition, jet generation, and recovery. The energy deposition stage is very important, as it determines the amount of electrical energy deposited into the cavity. The energy deposition efficiency is the product of the discharge efficiency and the heating efficiency. The former is the key factor under a certain input energy, while the latter is mainly determined by the voltage waveform, such as microsecond or nanosecond high voltage. According to the previous study, the discharge efficiency can be improved by higher arc resistance [21]. Increasing the electrode distance can increase arc resistance. However, the distance is restricted by the voltage amplitude. As a result, the optimal solution is to increase the discharge channel distance without increasing the voltage amplitude. The other limitation is the small affected area as the cavity outlet orifice is on the order of millimeter in diameter. An array of PSJAs is desired for the application on a large scale aerodynamic surface. However, different from the barrier discharge, the resistance characteristic of the arc discharge channel is negative. As a result, it is difficult to generate large area arc discharge. Several power supplies are needed to drive the actuator array, which is apparently not feasible in practice. Tie et al. proposed a six channel spark discharge method [22]. However, the requirement of very high trigger voltage (40 kV) and very short rise time (25 ns) makes the idea far from application at current technological capability.

The present work is carried out to address the limitation of PSJA, namely increase efficiency and affected area. A multichannel discharge circuit based on voltage relay is proposed in this paper. It enables the concept of multichannel discharge plasma synthetic jet actuator (MD-PSJA). This concept is further developed into two forms, the multi-electrode PSJA (ME-PSJA) and multi-PSJA array. The proposed MD-PSJA is driven by just one power supply.

## **2. Experimental setup**

### **2.1 Multichannel discharge circuit**

The multichannel discharge circuit is shown in Fig. 1. A DC power supply (0-15 kV) is used to charge the capacitor C, namely the discharge capacitor. The resistor  $R_1$  (10 M $\Omega$ ) is the current limiting resistor. The key feature of the multichannel discharge circuit is the voltage relay using the parallel resistance and capacitor. The high voltage of the power supply charges the electrode couple in sequence, and the parallel resistance and capacitor work as the relaying partner. These discharge electrode couples are connected in series, and the parallel resistance and capacitor are served as the relaying partner. In detail, these discharge electrodes are connected in series, and each of them is grounded through a high resistance  $R_p$  and a little capacitor  $C_p$ . In this paper, the  $R_p$  and  $C_p$  are chosen as 1 M $\Omega$  and 100pF, respectively. The voltage and current measurement points are also labelled in Fig. 1.

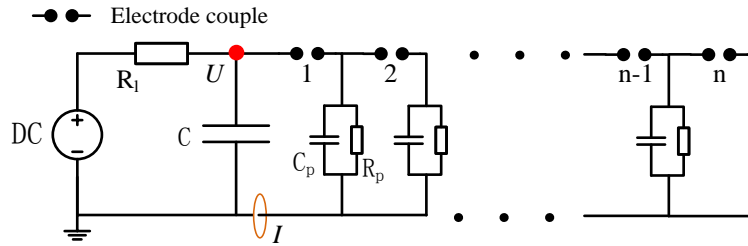


Fig. 1 The multichannel discharge circuit schematic diagram

## 2.2 Multichannel discharge plasma synthetic jet actuator

Two types of MD-PSJA, namely the ME-PSJA and the multi-PSJA array, are examined in this section. The former has several electrodes in one cavity, while the latter is comprised of several conventional PSJAs. Both types are driven by only one power supply.

An 11-electrode PSJA is shown in Fig. 2. The cavity volume is  $2651 \text{ mm}^3$ , and gap between two electrode pair is 2.6 mm. The diameter and depth of the orifice are 4 mm and 1 mm, respectively. With 11 electrodes, the distance of the total arc channel increases by 10 times. The arc resistance also increases. As a result, the discharge efficiency is expected to grow. Moreover, the heating volume in the PSJA cavity increases, which is also beneficial for the performance improvement.

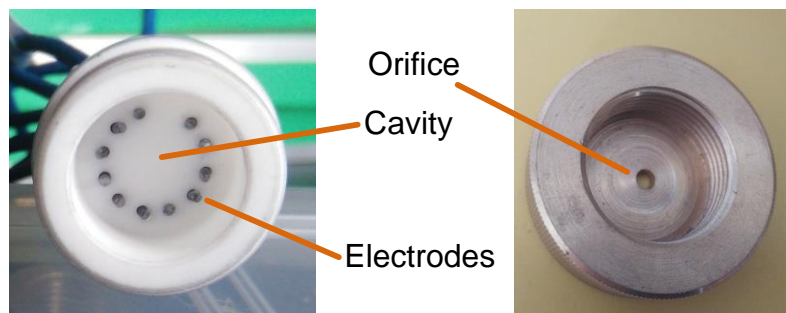


Fig. 2 The 11-electrode PSJA

The PSJA-array is consisted of 12 standard two electrodes PSJA in order to fit the field of view of the camera, as shown in Fig. 3. The cavity volume of one PSJA is  $503 \text{ mm}^3$ , and the electrode gap is 3 mm. The diameter and depth of the orifice are 2 mm and 1 mm, respectively.



Fig. 3 The 12 PSJAs array

## 2.3 Measurement systems

The discharge current and voltage waveforms are measured by a high voltage probe (Tektronix, P6015A) and a current probe (Pearson, 2878), respectively. An oscilloscope (Tektronix, DPO4014) with 1 GHz bandwidth is used to record the current and voltage.

The discharge image is captured with a Nikon D7000 camera, f-stop f/6.3, exposure time 1/320 s, ISO 100. Due to the large current limiting resistor, the discharge frequency is less than 10 Hz. Therefore, there is only one discharge for each image acquisition.

The flow field is visualized through schlieren imaging. A continuous bi-Xenon head lamp is used as light source. A high speed camera (PCO-dimax) is used to capture the images. In the experiment on the multichannel discharge evolution process, the frame rate and exposure time are 70028 Hz and 0.98

$\mu\text{s}$ , respectively. In the experiment on ME-PSJA, the frame rate and exposure time is 200000 Hz and  $0.83 \mu\text{s}$ , respectively. In the experiment on Multi-PSJA array, the frame rate and exposure time is 271002 Hz and  $0.77 \mu\text{s}$ , respectively. The detailed experiment description is can be found in reference [23].

### 3. Results and discussion

#### 3.1 Working process of the multichannel discharge circuit

The typical discharge voltage and current waveforms are shown in Fig. 4, which shows how the circuit works. Before the breakdown of the first electrode couple, the voltage across the capacitor  $C$  and the first electrode couple are almost the same. So the measured voltage can be used as the voltage across the first electrode couple. At about  $40 \text{ ns}$ , the voltage is higher than the breakdown threshold, and it causes breakdown of the first discharge couple. The current and the voltage then change dramatically throughout the breakdown process. It should be noted that the impedance characteristic of the first electrode couple transforms from a capacitor to a resistor during its breakdown. Therefore, the voltage across the next electrode couple increases to the voltage across the capacitor  $C$ . Due to the large resistance of  $R_p$  and the small capacitance of  $C_p$ , there is little change in the energy stored in the capacitor  $C$ , and the voltage across the next discharge gap increases to its breakdown threshold value. Benefitting from the parallel capacitor  $C_p$ , the discharge remains live until breakdown has happened in all electrode gaps. Consequently, as long as the breakdown voltage of the later electrode couple is not larger than that of the first electrode couple, the discharge channel can be built in sequence. As shown in Fig. 4, compared with the traditional discharge process<sup>[24]</sup>, there is an obvious breakdown stage in the discharge process. At  $700 \text{ ns}$ , breakdown happens in all electrode gaps. Afterwards, the discharge current increases quickly. It can be seen that the discharge process is similar to the traditional one channel discharge.

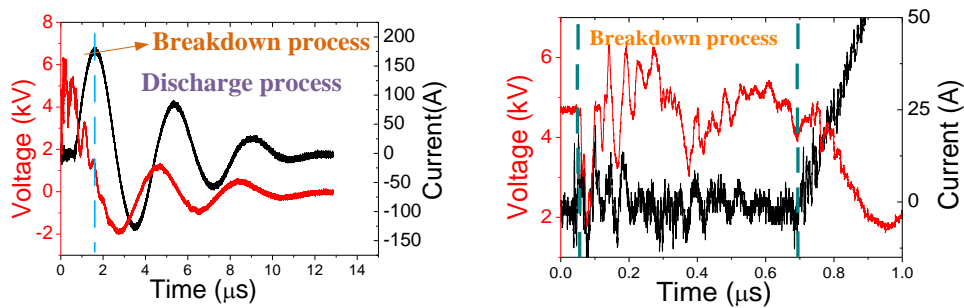


Fig. 4 The typical discharge waveform: (a) The whole process (b) The breakdown process

The multichannel discharge process is visualized by high-speed schlieren visualization system. 7 discharge channels are visualized in the present field of view, as shown in Fig. 5. When the breakdown happens in all electrode gaps, the bright arc is generated and the discharge current increases quickly. At around  $12 \mu\text{s}$ , the discharge process terminates. Since then, a strong shock wave appears. The white region in the center of the shock wave is the heating region. Although the discharge channel is built up in sequence, the gas dynamics evolution process of different discharge channel is almost the same, suggesting that as long as the electrodes gap distance is the same, the deposited energy in different channels is almost the same.

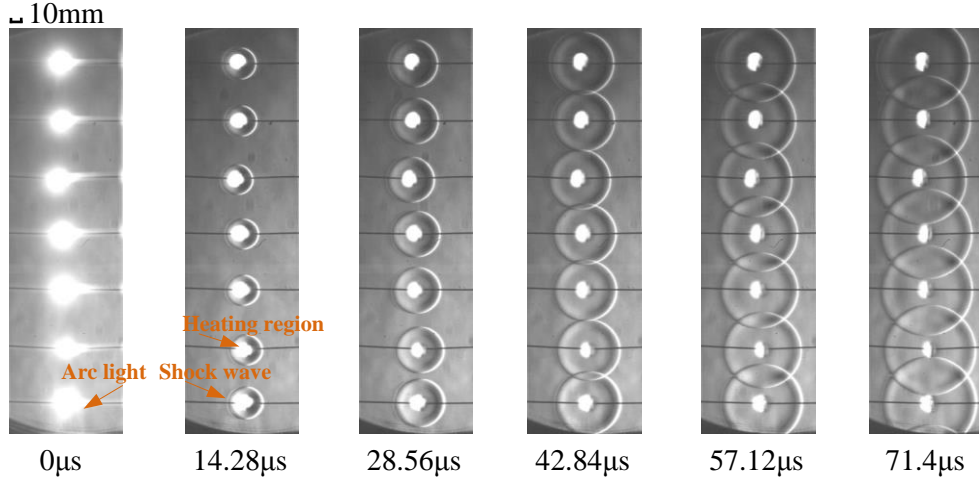


Fig. 5 The multichannel discharge evolution process

### 3.2 ME-PSJA

The discharge voltage and current waveforms of 2-electrode and 11-electrode PSJA are compared in Fig. 6. Assuming the plasma region as a constant resistor, the discharge circuit can be described as a standard resistor-inductor-capacitor circuit. Then the discharge current can be obtained be as following.

$$i_d(t) = A \cdot e^{-\alpha t} \cdot \sin(\omega t)$$

In this equation, parameters  $A$ ,  $\alpha$ , and  $\omega$  are determined by the circuit resistor, inductor, capacitor, and the initial voltage. The capacitor is fixed. The initial voltage is measured. As a result, the circuit resistor and inductor can be calculated by data fitting method.

The plasma resistance increases from  $0.61\Omega$  to  $6.41\Omega$ , when the number of discharge channel increases from 1 to 10. Since the wire resistance and equivalent series resistance of the discharge capacitor is about  $1.89\Omega$ . The discharge efficiency of 2-electrode and 11-electrode PSJA can be determined to be 25% and 77%, respectively. Therefore, the 11-electrode PSJA has much higher discharge efficiency. Moreover, the discharge voltage waveforms reveal that the breakdown voltage doesn't change with the increase of discharge channel.

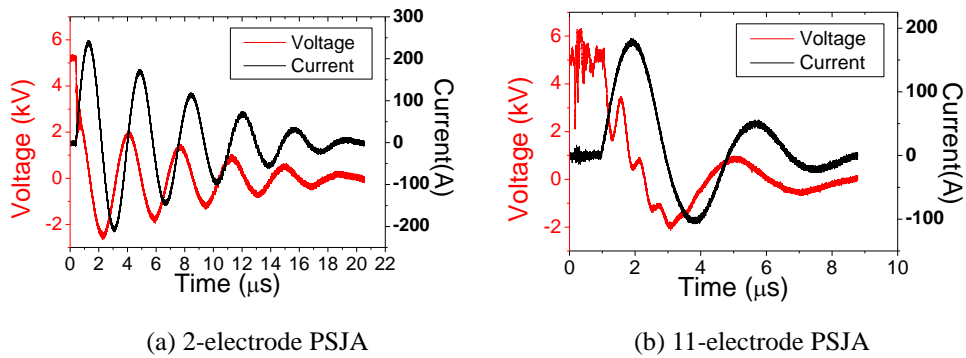


Fig. 6 The discharge voltage and current waveforms

This novel multichannel discharge circuit enables to increase the number of discharge channel without raising the voltage amplitude. The images of different discharge channels are shown in Fig. 7. The spark light intensity grows significantly when the number of discharge channel increases, suggesting that the deposited energy increases with increasing discharge channels. In this experiment, the capacitor  $C$  and DC voltage remain unchanged. Therefore, the energy efficiency increases.

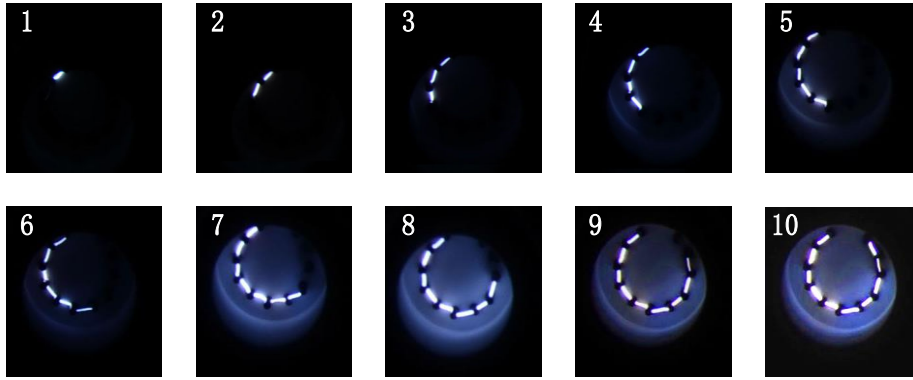


Fig. 7 The discharge images of different channels of the ME-PSJA

The schlieren images at  $502 \mu\text{s}$  with different number of discharge channels for the ME-PSJA are shown in Fig. 8. The number of discharge channel is labelled at the top left corner. The corresponding discharge images are shown in Fig. 7. The velocity of the jet front is estimated through the position of the jet front of two consecutive images. It is also labeled in Fig. 8. The jet velocity produced by the 11-electrode PSJA has velocity of  $142.1 \text{ m/s}$  while that of the conventional 2-electrode PSJA is only  $96.5 \text{ m/s}$ .

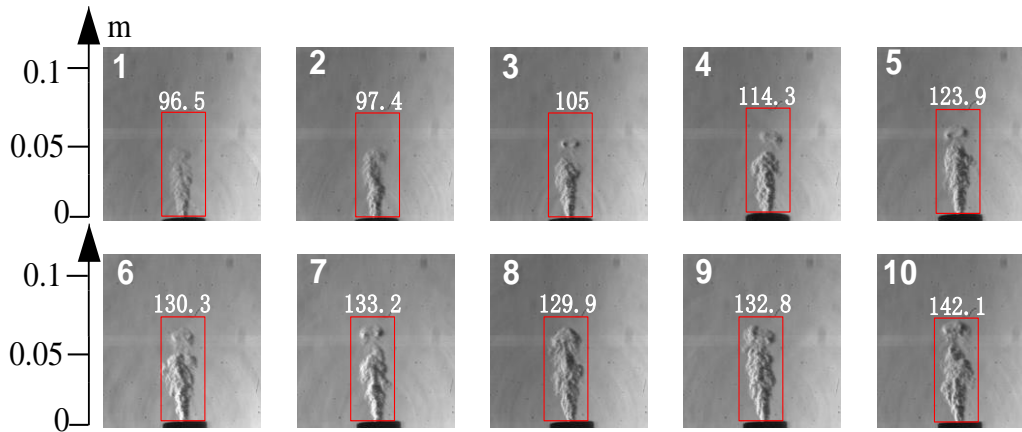


Fig. 8 The schlieren images at  $502 \mu\text{s}$  with different discharge channels of the ME-PSJA (unit of the jet front velocity is in m/s)

### 3.3 Multi-PSJA array

The schlieren image of the 12-PSJA array captured at  $151 \mu\text{s}$  is shown in Fig. 9, where the schlieren image of a single PSJA captured at  $151 \mu\text{s}$  is also included for comparison. Obviously, the affected area of the 12-PSJA array is larger than that of a single PSJA. Using the method described in reference [25], the total affected area of the 12-PSJA array is  $1.16\text{e-}5 \text{ m}^2$ , while the affected area of a single PSJA is just  $1.95\text{e-}6 \text{ m}^2$ . The affected area of the 12-PSJA array is almost 6 times of that of the single PSJA.

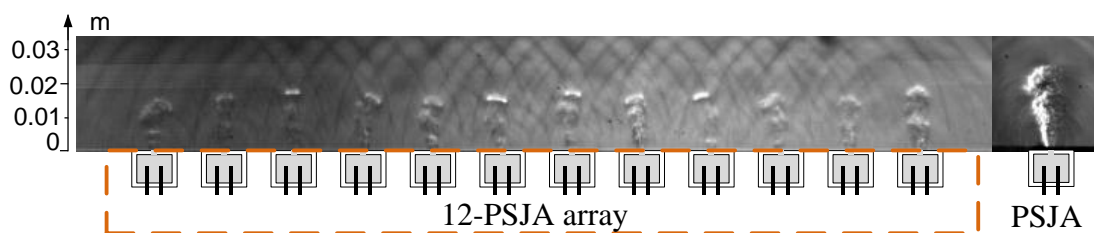


Fig. 9 The schlieren image of the multi-PSJA array captured at  $151 \mu\text{s}$

The jet front velocity of each PSJA in 12-PSJA array is shown in Fig. 10. The PSJA in the 12-PSJA array is numbered from left. As the PSJA is made through in-house fabrication, the performance of each PSJA is slightly different. The standard deviation of each jet velocity is 5.8 m/s, so it is believed the performance of individual PSJA in the array doesn't change significantly. The mean velocity for the 12-PSJA array is estimated to be 100 m/s, which is 64% of that produced by the single PSJA (157 m/s). However, this decrease in velocity is compensated by the enlarged affected area.

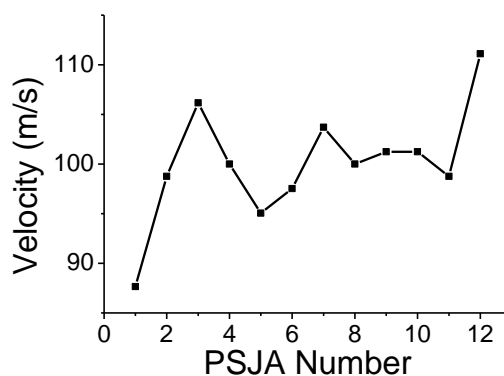


Fig. 10 The jet front velocity of different PSJA in the multi-PSJA array

#### 4. Conclusions

In order to improve the discharge efficiency and affected area of the PSJA, two types of MD-PSJA, which are ME-PSJA and multi-PSJA array, are put forward and experimental examined. The key feature of the multichannel discharge PSJA is the multichannel discharge circuit based on voltage relay using parallel resistance and capacitor. Discharge voltage and current waveforms reveal that the discharge efficiency of 11-electrode PSJA increases to 77%, which is 3 times of 2-electrode PSJA. Schlieren visualization shows that the 11-electrode PSJA leads to a 47% increase in the jet velocity with the same input energy compared with the 2-electrode PSJA. The 12-PSJA array driven by only one power supply system results in 6 times affected area and 64% jet velocity of a traditional PSJA. The MD-PSJA opens new prospects of the PSJA, and is worthy to be investigated in the future.

#### Acknowledgments

The authors would like to acknowledge the support by the National Natural Science Foundation of China (51522606, 51336011, 51611130198, 51407197 and 11472306) and Royal Society (IE150612).

#### Reference

- [1] Moreau E. Airflow control by non-thermal plasma actuators. *Journal of Physics D: Applied Physics*, 2007, 40(3): 605.
- [2] Li Y, Wu Y, Song H, et al. Plasma flow control. In: *Aeronautics and Astronautics*, Mulder, M. Ed., InTech: Croatia, 2011, 21-54.
- [3] Santhanakrishnan A, Reasor Jr D A, LeBeau Jr R P. Characterization of linear plasma synthetic jet actuators in an initially quiescent medium[J]. *Physics of Fluids (1994-present)*, 2009, 21(4): 043602.
- [4] Santhanakrishnan A, Jacob J. Characterization of linear spark jet actuators. AIAA 2008-538

- [5] Pescini E, Francioso L, De Giorgi M G, et al. Investigation of a micro dielectric barrier discharge plasma actuator for regional aircraft active flow control. *IEEE Transactions on Plasma Science*, 2015, 43(10): 3668-3680.
- [6] Debien A, Benard N, Moreau E. Streamer inhibition for improving force and electric wind produced by DBD actuators. *Journal of Physics D: Applied Physics*, 2012, 45(21): 215201.
- [7] Forte M, Jolibois J, Pons J, et al. Optimization of a dielectric barrier discharge actuator by stationary and non-stationary measurements of the induced flow velocity: application to airflow control. *Experiments in Fluids*, 2007, 43(6): 917-928.
- [8] Benard N, Mizuno A, Moreau E. A large-scale multiple dielectric barrier discharge actuator based on an innovative three-electrode design. *Journal of Physics D: Applied Physics*, 2009, 42(23): 235204.
- [9] Wang C C, Durscher R, Roy S. Three-dimensional effects of curved plasma actuators in quiescent air. *Journal of Applied Physics*, 2011, 109(8): 083305.
- [10] Liu A B, Zhang P F, Yan B, et al. Flow characteristics of synthetic jet induced by plasma actuator. *AIAA journal*, 2011, 49(3): 544-553.
- [11] Santhanakrishnan A, Jacob J. Effect of plasma morphology on flow control using plasma synthetic jet actuators. *AIAA 2007-783*.
- [12] Corke T C, Enloe C L, Wilkinson S P. Dielectric barrier discharge plasma actuators for flow control\*. *Annual review of fluid mechanics*, 2010, 42: 505-529.
- [13] Wang J J, Choi K S, Feng L H, et al. Recent developments in DBD plasma flow control. *Progress in Aerospace Sciences*, 2013, 62: 52-78.
- [14] Shin J, Narayanaswamy V, Raja L, et al. Characteristics of a plasma actuator in Mach 3 flow. *AIAA 2007-788*.
- [15] Cybyk B Z, Wilkerson J T, Grossman K R, et al. Computational assessment of the sparkjet flow control actuator. *AIAA 2003-3711*.
- [16] Cybyk B Z, Wilkerson J T, Grossman K R. Performance characteristics of the sparkjet flow control actuator. *AIAA 2004-2131*
- [17] Webb N, Clifford C, Samimy M. Control of oblique shock wave/boundary layer interactions using plasma actuators. *Experiments in fluids*, 2013, 54(6): 1-13.
- [18] Narayanaswamy V, Raja L L, Clemens N T. Control of unsteadiness of a shock wave/turbulent

- boundary layer interaction by using a pulsed-plasma-jet actuator. *Physics of Fluids* (1994-present), 2012, 24(7): 076101.
- [19] Narayanaswamy V, Raja L L, Clemens N T. Characterization of a high-frequency pulsed-plasma jet actuator for supersonic flow control. *AIAA journal*, 2010, 48(2): 297-305.
- [20] Golbabaei-Asl M, Knight D, Wilkinson S. Novel technique to determine sparkjet efficiency. *AIAA Journal*, 2014, 53(2): 501-504.
- [21] Zong H, Wu Y, Jia M, et al. Influence of geometrical parameters on performance of spark jet actuator. *Journal of Physics D: Applied Physics*, 2016, 49: 025504
- [22] Tie W, Liu X, Liu S, et al. Experimental Study on the Multichannel Discharge Characteristics of a Multi-Plasma-Jet Triggered Gas Switch. *IEEE Transactions on Plasma Science*, 2015, 43(4): 937-943.
- [23] Zong H, Wu Y, Song H, et al. Investigation of the performance characteristics of a plasma synthetic jet actuator based on a quantitative Schlieren method. *Measurement Science and Technology*, 2016, 27(5): 055301.
- [24] Zhang Z, Wu Y, Jia M, et al. Influence of the discharge location on the performance of a three-electrode plasma synthetic jet actuator. *Sensors and Actuators A: Physical*, 2015, 235: 71-79.
- [25] Zong H, Cui W, Wu Y, et al. Influence of capacitor energy on performance of a three-electrode plasma synthetic jet actuator. *Sensors and Actuators A: Physical*, 2015, 222: 114-121.